

Analytical framework for Adaptive Compressive Sensing for Target Detection within Wireless Visual Sensor Networks

Salema Fayed · Sherin M.Youssef ·
Amr El-Helw · Mohammad Patwary ·
Mansour Moniri

Received: date / Accepted: date

Abstract Wireless visual sensor networks (WVSNs) are composed of a large number of visual sensor nodes covering a specific geographical region. This paper addresses the target detection problem within WVSNs where visual sensor nodes are left unattended for long-term deployment. As battery energy is a critical issue it is always challenging to maximize the network's lifetime. In order to reduce energy consumption, nodes undergo cycles of active-sleep periods that save their battery energy by switching sensor nodes ON and OFF, according to predefined duty cycles. Moreover, adaptive compressive sensing is expected to dynamically reduce the size of transmitted data through the wireless channel, saving communication bandwidth and consequently saving energy. This paper derives for the first time an analytical framework for selecting node's duty cycles and dynamically choosing the appropriate compression rates for the captured images and videos based on their sparsity nature. This reduces energy waste by reaching the maximum compression rate for each dataset without compromising the probability of detection. Experiments were conducted on different standard datasets resembling different scenes; indoor and outdoor, for single and multiple targets detection. Moreover, datasets were chosen with different sparsity levels to investigate the effect of sparsity on the compression rates. Results showed that by selecting duty cycles and dynamically choosing the appropriate compression rates, the desired performance

S. Fayed^{a*} · S. M.Youssef^a · A. El-Helw^b

^a Computer Engineering Department, ^b Electronics and Communication Department,
College of Engineering and Technology, AAST, Alexandria, Egypt

* E-mail: fw010203@student.staffs.ac.uk

M.Patwary^c

^c School of Computing and Digital Technology, Birmingham city University
Birmingham, B47XG UK

M. Moniri^d

^d School of Architecture, Computing and Engineering, University of East London,
London, UK

of detection can be achieved with adaptive CS and at the same time saving energy, where the proposed framework results in an 70% on average energy saving as compared to transmitting the captured image without CS.

Keywords Compressive sensing · Duty cycles · Target detection · Wireless visual sensor networks

1 Introduction

Due to the advancement of new technologies, there are immediate requirements for automated energy-efficient Wireless Visual Sensor Networks (WVSNs) applications. WVSNs have addressed various applications such as environmental monitoring, animal behavior, surveillance applications, law enforcement, industrial automation and military purposes. Visual sensor nodes are resource constraint devices bringing together the special characteristics of WVSNs such as energy, storage and bandwidth constraints that introduced new challenges [1–6]. Each visual sensor node is powered by an attached battery and embeds a visual sensor, digital signal processing unit, limited memory and a wireless transceiver. The visual sensor can be integrated with other types of sensors such as vibration and acoustic sensors. Energy utilization is necessary to maximize the network's lifetime due to the limited battery power and communication bandwidth.

This paper addresses the target detection problem within WVSNs where visual sensor nodes are left unattended for long-term deployment. Amongst the many diverse application domains of WSNs, object detection is one of the most important tasks in image processing applications. Object can be a human being, a vehicle or any targeted object. As battery energy is a critical issue, it is always challenging to maximize the network's lifetime by minimizing the energy consumption due to sensing, processing and transmission without compromising the detection performance. In order to reduce energy consumption, nodes undergo cycles of active-sleep periods that save their battery energy by switching sensor nodes ON and OFF, according to a predefined duty cycles.

At the same time, there is a scope to achieve the same energy saving by minimizing the volume of data required for target detection. WVSNs deal with large data sets of videos and still images resulting in high demand on memory space and higher complexity of data processing and analysis for the object detection problem which are all quite costly in terms of energy consumption, memory requirements as well as communication bandwidth demand for transmitting the large image data. To represent the captured data in such a way to save storage due to memory constraint, an adaptive Compressive Sensing (CS) technique is proposed to compress the data depending on the sparsity of different images. Consequently, it is expected that this technique will save bandwidth requirement for transmission and processing power. CS is a simple process where it enables simple computations to be executed at the encoder side (sensor nodes) and all the complex computations for recovery of images are left at the decoder side or receiver (not battery-powered). In addition to

energy, memory constraints and communication bandwidth, CS will not affect quality of image (as denoted by Peak signal-to-noise ratio (PSNR)) for later target detection. Adaptive CS dynamically chooses the compression rate according to the sparsity nature of frames that varies from one dataset to another. In contrast to static compression rates, different datasets have different sparsity levels, hence if the same dimension of the sensing measurement matrix is used for more sparse images, this will result in a waste of energy where more compression could have been applied. In the case of less sparse images, the quality after reconstruction will be affected. Therefore, dynamic size of sensing measurement matrices result in saving energy, space requirements, as well as channel bandwidth.

Due to many factors such as node deployment, number of nodes, velocity and position of targets, the performance of detection may degrade. Moreover, the impact of CS versus adaptive CS to reduce the size of transmitted data on the object detection problem for WWSNs is analyzed. As a result of integrating adaptive CS with the detection problem, the performance may feature further degradation than the desired and acceptable performance level. This is due to other factors such as image sparsity and, loss of information in compression. Hence, there is always a tradeoff between energy consumption (network lifetime) and detection performance. As a result, the main goal of this paper is to derive an analytical framework to examine the selection of sensor node's duty cycles and dynamically choosing compression rates for different images and videos. The idea is to maximize the network's lifetime and reduce the energy waste without compromising the probability of detection.

The rest of the paper is organized as follows, related work is discussed in Section 2. Introduction to CS is then presented in Section 3. Section 4 presents the proposed system model. The analytical framework is first derived in Section 5 to evaluate the probability of missed detection, then the impact of adaptive CS on the probability of missed detection is investigated. Simulations and results are presented and discussed in Section 6. Finally the conclusion and future work are summarized in Section 7.

2 Related work

As battery energy is a crucial issue, in [7] the authors addressed the target detection problem for long lasting surveillance applications using unattended WSNs. In this context, the authors distributed the processing on sensor nodes by switching ON and OFF according to proper duty cycles of the sensing and communication modules of wireless sensor nodes. Making these modules work in discontinuous fashion by random scheduling saves energy however, it has an impact on the detection problem. In order to maintain a given performance objectives, the authors derived an analytical framework to evaluate the probability of missed target detection. In [8], the authors adopted a model of unsynchronized duty-cycle scheduling for individual nodes. Where, nodes sleep and wake-up periodically, according to duty cycles by setting the length of the

duty cycle period and the percentage of time nodes are awake within each duty cycle. However, the wake-up times are not synchronized among nodes as random scheduling is probably the easiest to implement in sensor networks, since it requires no coordination among nodes. Moreover, coordination among nodes requires additional energy as it involves some message exchange. In contrast, random scheduling does not require communication, each node simply sets its own duty-cycle schedule according to the agreed-upon wakeup ratio. The authors derived an analytical framework for the detection problem under different parameters such as duty cycles, nodes sensing times and number of deployed nodes.

A node selection scheme is presented in [9], which gives full consideration to both the information utility for the quality of tracking and the remaining energy of nodes to determine the longevity of nodes. Each sensor node is responsible of computing the detection probability, whereas the optimal set of sensors perform target tracking by integrating partial estimations. The node selection is formalized as an optimization problem and solved by genetic algorithms to optimize the tradeoff between the accuracy of tracking and the energy cost of nodes. While in [10] energy conservation in target tracking is achieved using different methods, prediction-based scheme coupled with selective activation of nodes is one of such methods, where nodes are waked-up on-demand following the target path. Previous active nodes collaborate between each other to generate an accurate estimation of the target.

In [11], the authors integrated reactive mobility of sensor nodes to improve the target detection performance of WSNs. Sparsely deployed mobile sensors collaborate with static sensors and move in a reactive manner to achieve the required detection performance. Specifically, mobile sensors remain stationary until a possible target is detected.

In the context of CS, it is a useful imaging tool under various noise conditions when the underlying image is compressible in a known basis or representation. CS is a new paradigm for data acquisition and processing originally developed for the efficient storage and compression of digital images [12, 13], it has been widely used in several applications such as image processing, steganography and image watermarking [14, 15]. In [16], compressive sensing for background subtraction and multi-view ground plane target tracking are proposed. A convex optimization known as basis pursuit or orthogonal matching pursuit is exploited to recover only the target in the difference image using the compressive measurements to eliminate the requirement of any auxiliary image reconstruction. Other work in compressive sensing for surveillance applications has been proposed in [17], where an image is projected on a set of random sensing basis yielding some measurements, where at the receiver end the image is reconstructed by minimizing the weighted version of the L2 norm. However, further research is required to address the selection of the weights and fully understand their impact on the reconstruction problem while taking into account the energy-efficiency parameter.

Another promising direction is the adaptive CS in [18], where energy efficient data collection in WSN using adaptive compressive sensing is proposed.

An adaptive approach is proposed to select a routing path by choosing sensors required to transmit their data. However, in this approach adaptive CS is only applied for sensor nodes selection and no compression is performed on the transmitted data. A heuristic to solve the optimization problem (which is proven NP-hard) is proposed in [19] to find a sensing measurement matrix that maximizes the information gain per energy expenditure. It was shown that under suitable conditions, one can reconstruct an $(N \times N)$ matrix of rank r from a small number of its sampled measurements. This is done by solving an optimization problem, provided that the number of measurements is of order $N^{1.2r} \log n$, exact matrix recovery would be guaranteed with a reduced number of measurements. Subsequently, most existing work in adaptive compressive sensing use heuristic techniques which are computationally expensive, hence taking only into consideration the accuracy of the approximate data field while relaxing the energy constraint.

In [20], an adaptive block CS technique is proposed and implemented to represent the high volume of captured images for the purpose of energy efficient wireless transmission and minimum storage. Adaptive CS is expected to dynamically achieve higher compression rates depending on the sparsity nature of different datasets, while only compressing relative blocks in the image that contain the target to be tracked instead of compressing the whole image. Hence, saving power and increasing compression rates. Least mean square adaptive filter is used to predict the next location of the target to investigate the effect of CS on the tracking performance. The tracking is achieved in both indoor and outdoor environments for single/multi targets. Experiments were carried out to evaluate the performance of the adaptive CS and its effect on target detection and tracking. Results have shown that using adaptive CS, up to 20% measurements of data are required to be transmitted while preserving image quality. Moreover, for different datasets where the sparsity nature of each image differs, CS adaptively chooses the compression rates accordingly reaching a relation between the number of compressed measurements and ratio of non-zero pixels to the total number of pixels.

In summary, it is always a challenge to maximize the WWSN's lifetime without degrading the detection performance. There is no theoretical framework reported in the literature that addresses this problem. Hence, the aim of this paper is to derive an analytical framework to provide the intended detection performance with minimum energy requirement to obtain optimal utilization of energy. This is accomplished by analyzing the integration of selecting node's duty cycles using the probability density functions introduced in [8] and dynamically choosing the appropriate compression rates for captured images and videos, which are expected to reduce energy waste by reaching the maximum compression rate for each dataset without compromising the probability of detection. The adaptive compressive sensing scheme introduced in [20] proved that for a specific sparsity level a corresponding compression rate is required to guarantee image reconstruction with minimum mean square error (MSE) and approximately 33dB Peak signal to noise ratio (PSNR). Therefore, the aim is to derive an analytical framework integrating adaptive CS to the detection

problem and considering the resource constraints within WVSNs for target detection to evaluate the impact of energy saving due to visual sensor nodes' duty cycles. Moreover, to show that by choosing appropriate compression rates according to different sparsity levels of images, one can keep the same level of detection while reducing the size of transmitted images through the wireless channel which as a result increases the network's lifetime by saving energy that is one of the main constraints of wireless visual sensor networks (WVSN).

3 Compressive Sensing

According to Shannon-Nyquist sampling theory the minimum number of samples required to accurately reconstruct the signal without loss is twice its maximum frequency [21]. It is always challenging to reduce this sampling rate as much as possible, hence reducing the computation energy and storage. Within the scope of the authors knowledge, recently proposed CS [21] is expected to be a strong candidate to provide this and overcome the above mentioned limitations, where CS has been considered for different aspects of surveillance applications due to its energy efficient and low power processing as reported in [16, 22]. CS theory shows that a signal can be reconstructed from far fewer samples than required by Nyquist theory, provided that the signal is sparse (where most of the signal's energy is concentrated in few non-zero coefficients) or compressible in some basis domain [23]. CS is a simple and low energy consumption process which is suitable for power constraint sensor nodes, where complex computations are just done at the Base station (BS).

CS exploits the sparsity nature of frames, so it compresses the image using far fewer measurements. Although, it is not necessary for the signal itself to be sparse but compressible or sparse in some known transform domain Ψ according to the nature of the image (i.e., the original image has approximate sparse representations in some linear transformations), smooth signals are sparse in the Fourier basis, and piecewise smooth signals are sparse in a wavelet basis [12, 23–25].

Suppose an image ' \mathbf{X} ' of size $(N \times N)$ is K -sparse (where K is the number of non-zero elements) that either sparse by nature or sparse in some domain named Ψ domain, where Ψ is the basis invertible Orthonormal function of size $(N \times N)$ used to sparsify the image, driven from some transform such as the DCT, fourier, or wavelet, where $K \ll N$, that is, only K coefficients of \mathbf{X} are nonzero and the remaining are zero, thus the K -sparse image \mathbf{X} is compressible. CS then guarantees acceptable reconstruction and recovery of the image from lower number of samples (known as measurements) as compared to those required by shannon-Nyquist theory as long as the number of measurements M satisfies a lower bound defined in Eq.(1) which depends on how sparse the image is. Eq.(2) shows the mathematical representation of \mathbf{X} .

$$M \geq K \log(N/K) \ll N \quad (1)$$

$$\mathbf{X} = \Psi \mathbf{S} \quad (2)$$

Where, \mathbf{S} is a matrix containing the sparse coefficients of \mathbf{X} of size $(N \times N)$, The image is represented with fewer samples from \mathbf{X} instead of all pixels by computing the inner product between \mathbf{X} and a random sensing matrix known as Φ , namely through incoherent measurements \mathbf{Y} in Eq.(3), where Φ is of size $(M \times N)$ where $K \ll M \ll N$.

$\mathbf{y}_1 = \langle \mathbf{x}, \phi_1 \rangle$, $\mathbf{y}_2 = \langle \mathbf{x}, \phi_2 \rangle$, \dots , $\mathbf{y}_m = \langle \mathbf{x}, \phi_m \rangle$. Where $\phi_1, \phi_2 \dots \phi_m$ represent individual rows in ϕ

$$\mathbf{Y} = \Phi \mathbf{X} = \Phi \Psi \mathbf{S} = \Theta \mathbf{S} \quad (3)$$

Since $M < N$, recovery of the image \mathbf{X} from the measurements \mathbf{Y} is undetermined, However, if \mathbf{S} is K -sparse, and $M \geq K \log N$ it has been shown in [23] that \mathbf{X} can be reconstructed by ℓ_1 norm minimization with high probability through the use of special convex optimization techniques without having any knowledge about the number of nonzero coefficients of \mathbf{X} , their locations, neither their amplitudes which are assumed to be completely unknown a priori [12, 25, 26]

$$\min \|\hat{\mathbf{X}}\|_{\ell_1} \quad \text{subject to} \quad \Phi \hat{\mathbf{X}} = \mathbf{Y} \quad (4)$$

Convex optimization problem can be reduced to linear programming known as Orthogonal Matching Pursuit (OMP) which was proposed in [27] to handle the signal recovery problem. It is an attractive alternative to Basis Pursuit (BP) [13] for signal recovery problems. The major advantages of this algorithm are its speed and its ease of implementation. As seen, the CS is a very simple process as it enables simple computations at the encoder side (sensor nodes) and all the complex computations for recovery of frames are left at the decoder side or BS.

4 WVSN model

Consider a WVSN-based surveillance application model, composed of N visual sensor nodes randomly distributed over a specific geographical region as in Fig.1. Each sensor node is assumed to have a sensing radius r_s allocated to share a viewable range and fully cover the required geographical region, and one or more receiver/sink node at fusion center. The geographical region is assumed to be a square area with each side of size d_s . It is required to increase the WVSN's lifetime by reducing the energy consumption this is accomplished by periodically switching On and OFF the visual sensors. Each sensor node is assumed to be in 'wake-up' state according to a duty cycle $\beta_s \in [0, 1]$ over a period t_s , hence each sensor is awake for an interval of length $\beta_s t_s$ and sleep for an interval $(1 - \beta_s)t_s$ as shown in Fig,2.

During the sensor's ON interval, if the target is in the sensor's sensing area, it will take a snapshot of the scene and compress the image by applying adaptive CS. After the reconstruction of the image, the detection of the target is performed to examine if the integration of adaptive CS affected the

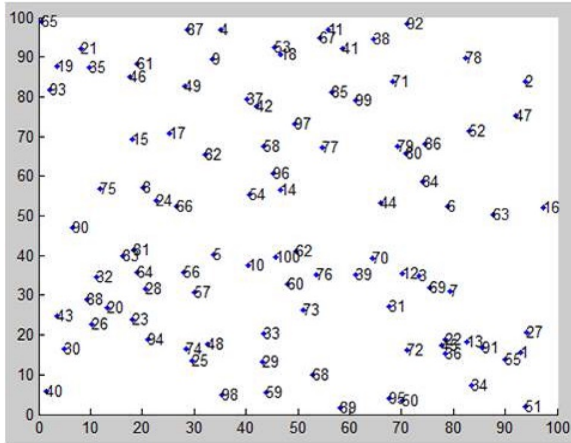


Fig. 1 Wireless visual sensor network

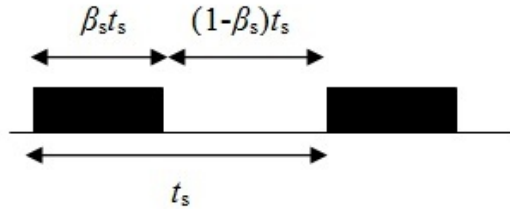


Fig. 2 Scheme for sensor's duty cycle

detection performance presented in [8]. Lets assume the following, the time reference for the frame count is assumed to be $t = 0$. Hence, a single snapshot at $t = 0$ is expected to be stored within the memory allocated at the sensor node; that is assumed to be the background for the intended target detection; will be denoted as \mathbf{X}_b . Following frames \mathbf{X}_t with $t > 0$ are subsequently captured frames in the video sequence, where \mathbf{X}_b and \mathbf{X}_t are of size $(N \times N)$. To achieve higher compression rates, the foreground target is extracted first by background subtraction resulting in the difference frame \mathbf{X}_d . Hence, assuring sparsity as the difference frame is always sparse regardless of the sparsity nature of original image frames. Within the image frame, the extraction of foreground target X_d is achieved at each sensor node, where CS is then applied producing the compressed measurements \mathbf{Y}_d for transmission through the wireless channel.

Adaptive CS is expected to reduce the size of sampled data by dynamically setting the size of sensing measurement matrices according to the sparsity nature of different datasets. For any given dataset, different M and Φ are needed, the value of M is inversely proportional to the degree of sparsity of an image. If the same dimension of the sensing measurement matrix M

is used for all different datasets, for more sparse images this will result in a waste of energy, where more compression rates could have been applied. And for less sparse images, the quality after reconstruction will be affected which in return degrades the detection performance. As a result, dynamic size of sensing measurement matrices result in saving energy, space requirements, as well as channel bandwidth. It is expected that the reliability of target detection will be different as the degree of sparsity varies from one image to another, for this reason there is a great challenge for adaptive CS by making the dimension of M variable depending on how sparse the image is. For the adaptive CS, the traditional CS process is preceded by a calibration phase. During that phase an Automatic Repeat Query (ARQ) transmission protocol is used between sensor nodes and the receiver side, as feedback is needed for the adaptation phase. A dictionary is constructed for different values of M and corresponding sensing matrices Φ . For each dataset the sparsity level is calculated by finding the ratio between the number of non-zero pixels and the total number of pixels in a frame. At the end of each adaptation/calibration phase, the dictionary is updated with the chosen M and Φ for the equivalent sparsity level that can be used later for other datasets with the same sparsity levels. Initially, an arbitrary value of M is chosen according to a sparsity measure and is used to obtain the compressed measurements \mathbf{Y}_d . The sensor node is then set to transmit \mathbf{Y}_d to the receiver side, where the image is to be reconstructed, and based on the reconstruction mean square error which is used as a performance indicator, a decision is made whether the reconstruction is satisfactory or not. In case the reconstruction results are satisfactory, the receiver node sends a 'zero' flag through the feedback channel, ending the calibration phase; otherwise a 'one' flag is to be sent. While the sensor node receives a 'one' flag, it is expected to change the value of M and change Φ accordingly, the sensor node repeats the search for an optimum value of M at the CS adaptation process till it receives a zero feedback from the receiver. At this point, the optimum values for M and Φ obtained are used next in the CS process.

At the receiver side, the received compressed data is to be decompressed for the reconstruction and recovery of the estimated data $\hat{\mathbf{X}}_d$. As mentioned, \mathbf{X}_b is known to the receiver making it possible to estimate and reconstruct the original test frame denoted as $\hat{\mathbf{X}}_t$ by adding \mathbf{X}_b after masking the target's locations in the background image to $\hat{\mathbf{X}}_d$. Finally, the system detects moving targets. The system model of the proposed work for the WWSN-based surveillance application is shown in Fig.3.

There is always a tradeoff between energy consumption (network lifetime) and detection performance, in the following subsection the probability of missed detection due to the sleeping theme and the integration of adaptive CS is described.

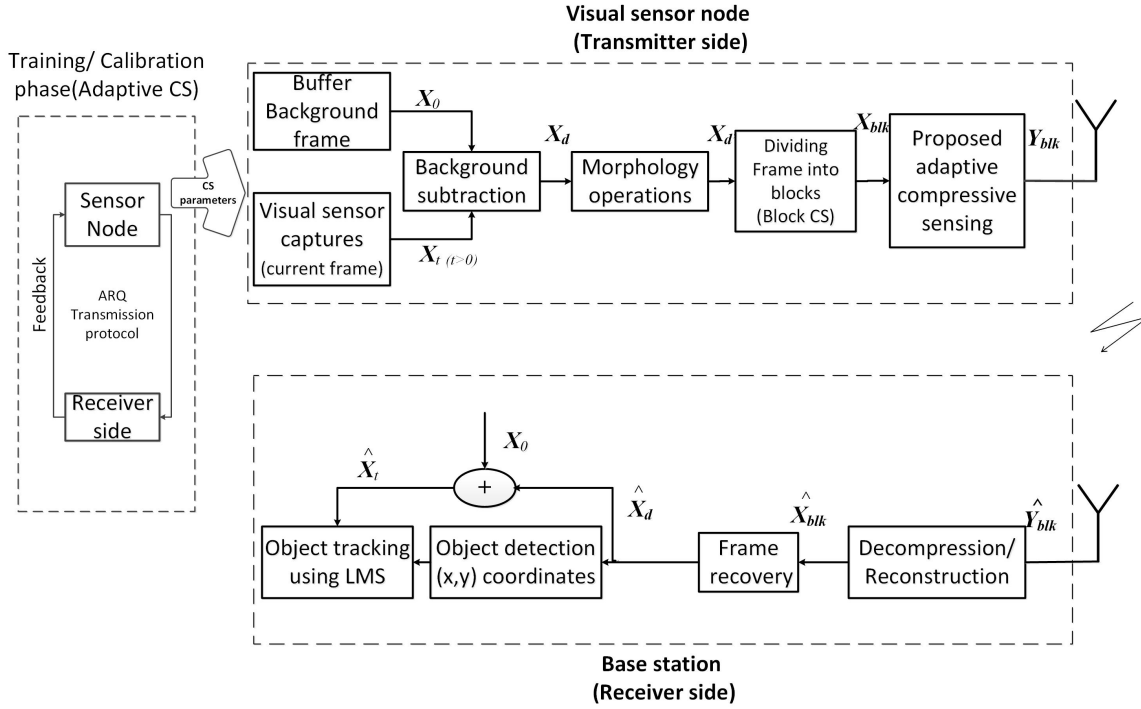


Fig. 3 The proposed model for WWSN-based surveillance application

5 Probability of missed detection

In subsequent sections an analytical framework is derived, first to evaluate the probability of missed detection as a function of the target's mobility model due to the predefined duty cycles. Second, the probability of missed detection is derived after the integration of adaptive CS to compare the performance of detection with and without CS.

5.1 Probability of missed detection as a function of mobility model of the target

In order to detect a target in a squared geographical area, N sensors are randomly deployed and set to periodically switch ON and OFF according to a predefined duty cycle β_s . To evaluate the probability of missed detection P_{md} , it is required to integrate the sensor's duty cycle. Assume that the target enters the sensing area at time t_a with angle θ and velocity v m/s crossing the sensing area in $T_{cross} = L/v$ where L is the length of intersection between the target's trajectory and the sensing area r_s as shown below in Fig.4,

To find the probability of missed detection, assume that ξ_{target} is the event, where the sensor is ON when the target enter the sensing area, and for a given

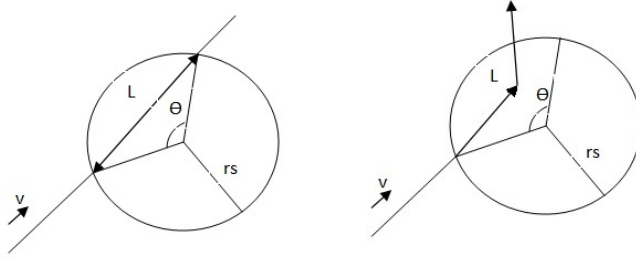


Fig. 4 Sensor model for (a) linear and (b) non-linear target trajectory

geographical area, N visual sensor nodes are distributed to cover this area. So, ξ_{target} describes the presence of a target in the required sensing area at the time where a given sensor is ON. ξ_{det} is the event where the sensor is ON when the target crosses the sensor's sensing area, so the target is detected by the given sensor. During a single time interval t_s , any incoming target entering a sensor's sensing area at time T_a during the interval $\beta_s t_s$ (i.e. the sensor is ON) will be detected. However, in the case where T_a is during the interval $(1 - \beta_s)t_s$ (i.e. during the sensor's sleep interval), in order to successfully detect the target, the target must remain in the sensing area till the sensor's next duty cycle where it turns ON again. Hence, the Probability of detection P_d is defined as in [8] by the total probability theorem as:

$$P_d = P\{\xi_{det}|\xi_{target}\}P\{\xi_{target}\} + P\{\xi_{det}|\bar{\xi}_{target}\}P\{\bar{\xi}_{target}\} \quad (5)$$

Where, $P\{\xi_{det}|\xi_{target}\} = 1$, $P\{\xi_{target}\} = \beta_s$, and $P\{\bar{\xi}_{target}\} = (1 - \beta_s)$, the last term $P\{\xi_{det}|\bar{\xi}_{target}\}$ in (5) denotes the case where the target is detected given it enters the sensing area during the sensor's sleep interval $(1 - \beta_s)t_s$. This suggests that either the target's crossing time $T_{cross} > (1 - \beta_s)t_s$, as a result, the target is detected, or the case where $T_{cross} < (1 - \beta_s)t_s$, in this case the target will only be detected if it enters the sensing area during the last part of the sleep interval, such that the target remains in the sensing area till the sensor turns ON in the next duty cycle. Hence, as in [8] $P\{\xi_{det}|\bar{\xi}_{target}\}$ is calculated in terms of the joint probability density function (pdf) as follows:

$$P\{\xi_{det}|\bar{\xi}_{target}\} = \int \int_D f_{T_a T_{cross}}(t, \tau) dt d\tau \quad (6)$$

where D is the integration domain described in [8, 28], $f_{T_a T_{cross}}(t, \tau)$ is the probability density function expressed as:

$$f_{T_a T_{cross}}(t, \tau) = \begin{cases} \frac{v}{\pi c \sqrt{r_s^2 - (\frac{v\tau}{2})^2}} & \text{if } 0 < \tau < 2r_s/v, 0 < t < c \\ 0 & \text{else} \end{cases} \quad (7)$$

where $\Pi \approx 3.14159$ and $c = (1 - \beta_s)t_s$ is the time interval where the target enters the sensing area, hence:

$$P\{\xi_{det}|\bar{\xi}_{target}\} = \begin{cases} \frac{4r_s}{\pi cv} & \text{if } 2r_s/v < c \\ \frac{4r_s - 2\sqrt{4r_s^2 - c^2v^2}}{\pi cv} + 1 - \frac{2 \arcsin(\frac{cv}{2r_s})}{\pi} & \text{else} \end{cases} \quad (8)$$

Finally, the P_d is written as:

$$P_d = \beta_s + (1 - \beta_s)P\{\xi_{det}|\bar{\xi}_{target}\} \quad (9)$$

Taking into consideration the independence of the N randomly deployed sensor nodes, the probability of missed detection can then be evaluated as:

$$P_{md} = (1 - P_d)^N \quad (10)$$

$$P_{md} = (1 - [\beta_s + (1 - \beta_s)P\{\xi_{det}|\bar{\xi}_{target}\}])^N \quad (11)$$

5.2 Probability of missed detection as a function of Compressive Sensing

Integrating CS to reduce the size of transmitted information to the target detection problem might lower the detection performance, as M the size of compressed measurements must be $M \geq K \log(N/K)$, where, the captured image is $(N \times N)$ and K is the number of non-zero pixels (which defines the sparsity level of the image). Hence, if M is chosen according to this bound the target will be detected with high probability. Moreover the performance of the detection problem is directly proportional to the PSNR of the image after reconstruction. First, probability of detection using CS $P_{d_{cs}}$ is calculated subject to the constraint that the probability of false alarm $P_{FA} \leq \alpha$ as in [29, 30].

$$P_{d_{cs}} = Q(Q^{-1}(\alpha) - \sqrt{M/N} \sqrt{PSNR} / \sqrt{K/N}) \quad (12)$$

Where, $Q(x) \triangleq \int_x^\infty e^{-t^2/2} dt$ is the complementary error function of x . This gives a way to measure how much information is lost after the reconstruction, not in terms of the reconstruction error of the image, but in terms of the ability to detect the target. To reach an acceptable $P_{d_{cs}}$, Φ is dynamically chosen according the sparsity nature of the image but without relaxing the randomness property of the projection sensing measurement matrix. Thus the size of Φ ($M \times N$) will be adaptively changing with respect to K .

Afterwards, the total probability of detection will be evaluated by integrating adaptive CS to the detection problem. Hence, the total probability of detection P_{d_t} becomes as follows:

$$P_{d_t} = (\beta_s + (1 - \beta_s)P\{\xi_{det}|\bar{\xi}_{target}\})P_{d_{cs}} \quad (13)$$

Resulting in a total probability of missed detection $P_{md_{CS}}$:

$$P_{md_{CS}} = (1 - [(\beta_s + (1 - \beta_s)P\{\xi_{det}|\bar{\xi}_{target}\})P_{d_{cs}}])^N \quad (14)$$

To maintain a high probability of detection P_{d_t} and a required PSNR while given the target's velocity, sparsity level of the image and sensing radius. One can dynamically find the best value for M that suits these requirements as in (16) by solving the following:

$$\hat{P}_{d_{cs}} = \begin{cases} \frac{P_{d_t} 4d_s \pi cv}{(2\pi r_s)(\beta_s \pi cv) + 4r_s - 4r_s \beta_s} & \text{if } 2r_s/v < c \\ \frac{P_{d_t} 4d_s}{2\pi r_s Z} & \text{else} \end{cases} \quad (15)$$

$$\text{Where } Z = \beta_s + (1 - \beta_s) \left(\frac{4r_s - 2\sqrt{4r_s^2 - c^2 v^2}}{\pi cv} + 1 - \frac{2 \arcsin(\frac{cv}{2r_s})}{\pi} \right)$$

$$M = \frac{(Q^{-1}(\alpha) - Q^{-1}(\hat{P}_{d_{cs}}))^2 k}{PSNR} \quad (16)$$

5.3 Probability of missed detection for multi-target detection scenario

The analysis of the detection problem is extended to consider the case of multiple targets entering the monitoring area. In this case it will be useful to evaluate the probability of missing all targets or missing at least one of the incoming targets. Assume N_T is the number of incoming targets and the probability of missing all incoming targets is denoted as P_{ma} and since the incoming targets are independent, then it can be evaluated as follows:

$$P_{ma} = (P_{md_{CS}})^{N_T} \quad (17)$$

Where $P_{md_{CS}}$ is the probability of missed detection in the case of single target detection after the integration of CS. The probability of missing at least one of the N_T , denoted as P_{mo} is expressed as

$$P_{mo} = 1 - (1 - P_{md_{CS}})^{N_T} \quad (18)$$

6 Analysis and discussion

6.1 Duty cycle analysis

The performance of the duty-cycled WWSN is characterized in terms of probability of missed target detection. The effect of different values of β_s are examined by testing the probability of detecting a given target as changing the value of β_s is expected to affect the detection problem, when β_s becomes small, the target can cross the sensed area, during a sleeping interval of a sensor resulting in missing a target. The detection performance has been tested under several parameters; different values of sensing times t_s , duty cycles β_s , sensing areas and number of sensor nodes N . All sensors are assumed to have the same sensing area r_s , and targets enter the monitored area with the same velocity v .

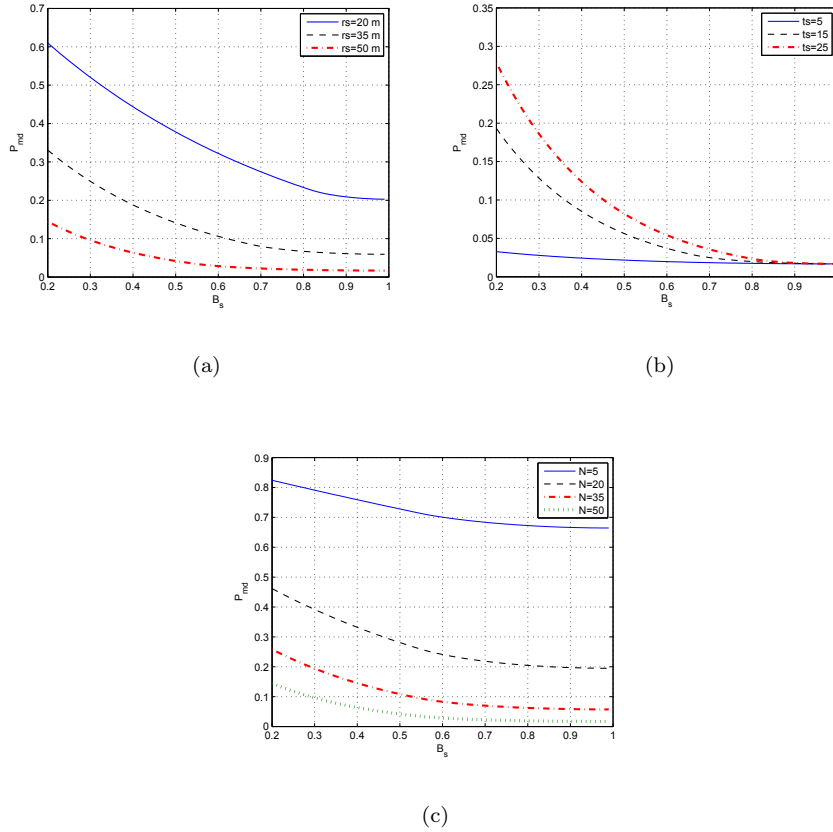


Fig. 5 Probability of missed detection vs. different duty cycles for (a) different r_s ($t_s = 15\text{sec}$, $N = 50$), (b) different t_s ($N = 50$, $r_s = 50$) and (c) different number of sensor nodes ($t_s = 15\text{sec}$, $r_s = 50$). In all cases the target enters with velocity $v = 15\text{m/s}$

6.2 Analysis of Probability of missed detection for duty-cycled WWSN

Analysis are carried out to address the target detection problem after applying sensors duty cycles and to evaluate the probability of missing a target under various parameters; t_s , β_s , sensing areas and number of sensor nodes N .

Fig.5 shows the P_{md} as a function of β_s for various values of r_s , t_s and sensor nodes N , in all cases the target's velocity is 15m/s . As illustrated, for lower values of β_s , there is a high chance the target enters and crosses the sensed area during the sleeping interval of the sensor, resulting in higher probability of missed detection. As β_s increases, the sensor node stays on for a longer time, decreasing the probability of missing a target. In Fig.5(a), the P_{md} is evaluated for different r_s , while t_s is set to 15sec and N to 50 nodes.

As shown, for larger sensing areas, the higher the probability of detecting the incoming target.

In Fig.5(b), P_{md} is shown for different values of t_s , while r_s and N are set to 50. It is clear from the figure that for lower values of t_s , the lower the probability of missed detection and the lower the impact of β_s on the detection problem, where the total sensing period t_s is short and sensors switch to the ON state more often. While for longer t_s , β_s has a direct impact on the probability of missing a target, as β_s becomes small, the probability a target crosses the sensing area while the sensor is in the OFF state gets higher leading to a higher P_{md} . In contrast, when β_s approaches 1 (sensors remain ON), the P_{md} converges for different values of t_s as the effect of t_s on the probability of detecting a target becomes negligible.

The impact of different numbers of sensor nodes on P_{md} is illustrated in Fig.5(c), where t_s is set to 15sec and r_s to 50. As shown, as N increases, the P_{md} decreases which explains that by deploying more sensors in the monitoring geographical area the higher the chance to guarantee more sensing coverage hence reducing the probability a target is missed. On the other hand, if fewer sensors are deployed, the probability a target enters a non-coverage area is high, as a result the probability the target is missed is higher. Fig.6 shows the P_{md} as a function of β_s for $N = 1$ and different values of r_s , there is significant increase in $P_{md} > 90\%$ even the effect of increasing the sensing area on the target detection problem becomes significantly low.

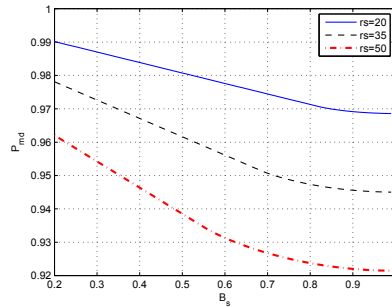


Fig. 6 Probability of missed detection vs. different duty cycles for $N = 1$ and different r_s , $t_s=15\text{sec}$ and the target enters with velocity $v = 15\text{m/s}$

Another important parameter that has a direct impact on P_{md} is the target's velocity when crossing the sensing area which in return also affects the time required by the target to cross a given sensing area T_{cross} . In Fig.7, P_{md} is analyzed as a function of β_s for different values of v while other parameters are kept constant ($N = 50$, $t_s = 15\text{sec}$, $r_s = 50$). For small values of β_s (the sensor is ON for short intervals) there is a high impact of v on P_{md} , where P_{md} increases as the target's velocity increases. The higher the velocity of the target crossing the sensing area, the shorter the time where the target crosses

the sensing area T_{cross} and as a result the target might cross the sensing area during a sensor's sleeping interval hence resulting in higher P_{md} . On the other hand, for lower velocities, the target crosses the sensing area for T_{cross} long enough so that any sensor on the target's trajectory will detect it even if the sensor is in sleeping mode when the target enters its sensing area, there will be a high probability the sensor turns ON before the target leaves its sensing area. As β_s approaches 1, target's velocity v has a limited impact on the detection performance and P_{md} converges to reach a lower bound.

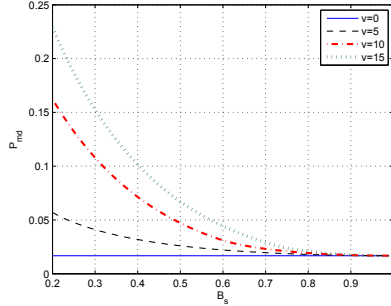


Fig. 7 Probability of missed detection vs. different duty cycles for different target's velocity ($N = 50$, $r_s = 50$, $t_s = 15sec$)

Fig.8 shows the P_{md} as a function of β_s for various values of r_s and v set to $100m/s$, N to 50 and t_s to $15sec$. As stated above, higher velocities result in higher probability of missing a target specially during short β_s duty cycles as the target crosses the sensing area in a short interval of time (the case where the sensor is OFF when target enters a sensing area and target leaves the sensing area before the sensor turns On again). However, the impact of high velocities could be eliminated by longer β_s and larger r_s , to increase the probability the target remains in the sensing area for a longer interval of time till detected. This is reflected in the figure, where for a $100m/s$ velocity the P_{md} decreases as r_s and β_s increases.

6.3 CS Simulation

All analysis previously presented were carried out to address the target detection problem after applying sensor's duty cycles and to evaluate the probability of missing a target under various parameters. Next, the probability of missing a target is reevaluated after the integration of adaptive CS with the detection problem. The advantages of adaptive CS to conventional CS will be illustrated in terms of energy saving and detection performance. First, to illustrate the relation between the number of compressed measurements required for CS to guarantee reconstruction and how sparse the image is, experiments are performed on different schemes resembling both indoor and outdoor schemes from

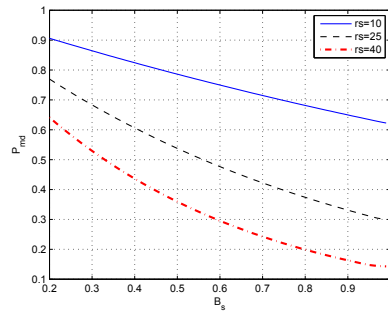


Fig. 8 Probability of missed detection vs. different duty cycles for different r_s , $v=100\text{m/s}$, $t_s = 15\text{sec}$, $N=50$

standard datasets chosen with different sparsity levels to investigate the effect of sparsity on the compression rates and how dynamically compression rates are selected to evaluate the performance of adaptive CS by choosing appropriate compression rates depending on sparsity nature of images; "Walking men" is chosen for dataset "1" to resemble an outdoor scene for multi target captured by [31]. While "Shopping center 1" and "Shopping center 2" for indoor scenes with different sparsity levels, tracking a single target from two different views; top view with a wide angle lens camera and a corridor side view, for dataset "2" and dataset "3" respectively, filmed for the EC funded CAVIAR project (CAVIAR is a project of the European Commission's Information Society Technology program found in [32]). "Walking" for dataset "4" resembles an outdoor scene with a street view for cars and targets tracking from PETS surveillance datasets [33], and according to the application, specific objects (cars or pedestrians) will be detected. Fig.9 shows samples from different datasets and the corresponding detected target. Next, we show the probability of detection by applying CS for various compression rates. Then, the impact of CS on the total probability of missed detection is illustrated.

Mean square error (MSE) and peak signal to noise ratio (PSNR) are used as performance indicators to test the reliability of CS. MSE and PSNR are compared for different number of CS measurements M , where the MSE is the reconstruction error measured between real and reconstructed frames and PSNR is measured after frames recovery to reflect the quality of image reconstruction, which will later reflects the ability of reliable tracking. The background frame and Φ are known to the receiver node. Two candidate sensing matrices have been compared; normally distributed random numbers using Matlab function "randn" and a walsh-hadamard. Although the measurements are defined by a matrix multiplication, the operation of matrix-by-vector multiplication is seldom used in practice, because it has a complexity of $O(MN)$ which may be too expensive for real time applications. When a randomly permuted Walsh-Hadamard matrix is used as the sensing matrix, the measurements may be computed by using a fast transform which has complexity of $O(K \log(N))$ [34]. The Hadamard matrix, is an $(N \times N)$ square matrix whose

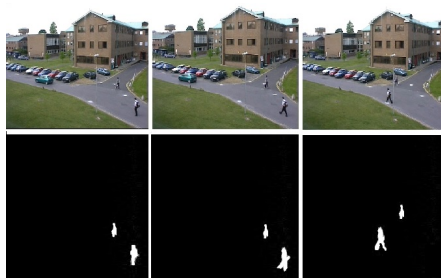


(a) dataset "1" Walking Men

(b) dataset "2" Shopping center 1



(c) dataset "3" Shopping center 2



(d) dataset "4" Walking

Fig. 9 First row in (a)(b) (c) and (d) shows test frames from different datasets and detected targets in second row

entries are either +1 or -1 and whose rows are mutually orthogonal, the matrix is first randomly reordered then, M samples are randomly chosen to construct the $(M \times N)$ random sensing matrix Φ .

6.3.1 Target Detection

The ability of reliable detection depends on acceptable recovery of images. In other words, if CS fails in image reconstruction the location of targets can not be detected. Hence, M is adaptively chosen depending on the sparsity nature of images as choosing the right value of M is critical in image reconstruction and afterwards detection. It is clear from the results in Fig.10, 11 and 12,

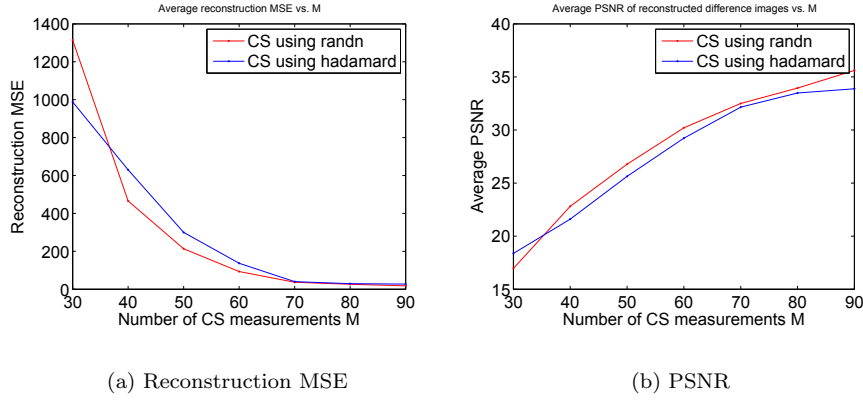


Fig. 10 Comparing reconstruction MSE and PSNR using randn and walsh sensing matrices for "Walking men" with $K=30\%$

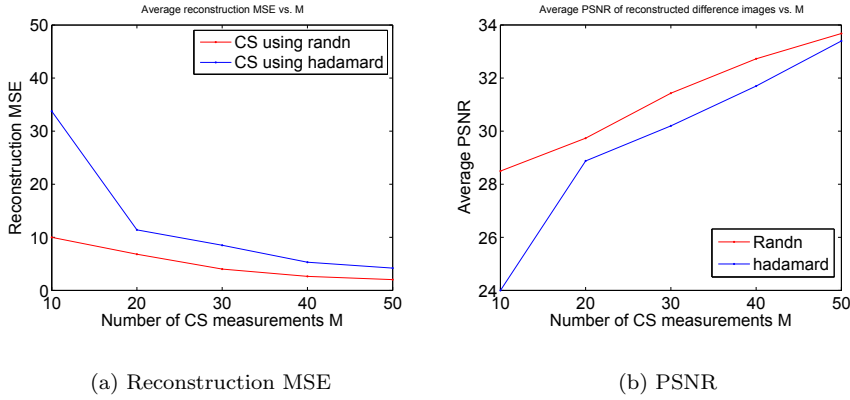


Fig. 11 Comparing reconstruction MSE and PSNR using randn and walsh sensing matrices for "Shopping center 1" with $K=3\%$

that for different sparsity levels $K = 30\%, 3\%$ and 11% respectively, different values of M and compression rates are required. When reaching optimum value of M , least MSE and $33dB$ PSNR are successfully achieved. For illustration, MSE decreases and PSNR increases as M increases till reaching the optimum value, it has been shown that the lower bound on M is dependent on how sparse the difference frame X_d is or in other words proportional to the ratio between the number of non-zero coefficients and the total number of pixels in a frame. For "Walking men", CS sets M to 70 as in Fig.10(a) to achieve satisfactory results. While for "Shopping center 1" and "Shopping center 2", it is obvious from Fig.11(a) and Fig.12(a) respectively, that for single-target tracking (where there is lower number of non-zero coefficients), better MSE is

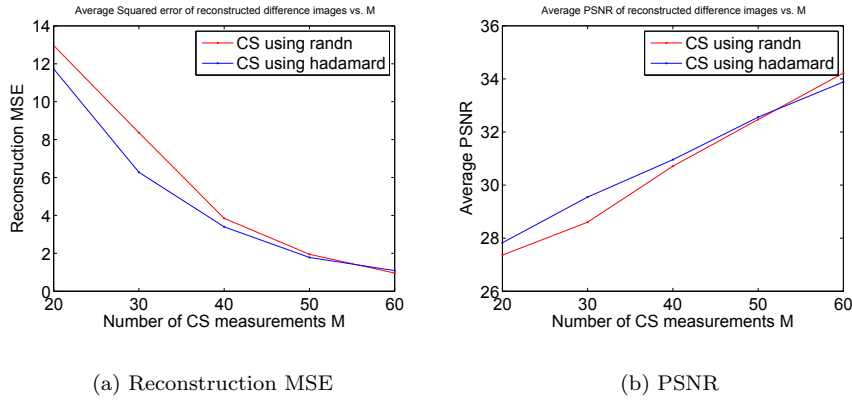


Fig. 12 Comparing reconstruction MSE and PSNR using randn and walsh sensing matrices for "Shopping center 2" with K=11%

achieved with lower M , reduced to 50 and 60 for Shopping center "1" and "2" respectively compared to multi-target tracking while maintaining least MSE and 33dB PSNR. As a result, making CS adaptive helps in increasing the compression rate and also avoiding the waste of using a higher value of M at the times where the image is sparse allowing for lower M . The above discussion reflects the reduction in channel bandwidth using CS by 72%, where instead of transmitting the whole (256×256) image, the compressed measurements of size (70×256) are transmitted. Whereas for more sparse images the reduction reaches 82% of the total image size.

CS states that when enough measurements are used for compression, the reconstruction is done with high accuracy depending on a lower bound of M . Trajectory tracking of moving targets is considered to reflect the degree of reconstruction accuracy and how accurate the target is detected. For different datasets according to sparsity levels, M is dynamically chosen based on adaptive CS, Fig.13 shows the (x,y) position plots of the path tracked for the targets in the camera's scene after CS reconstruction. It illustrates how the trajectory of the tracked targets after the CS reconstruction matches those of the real frame before compression.

Fig.14 shows trajectory tracking for multi targets for dataset "4" "Walking" after undergoing the different phases; detection, CS and reconstruction.

The above experiments were carried out using two different sensing matrices, Randn and walsh-Hadamard. They are compared with respect to MSE and PSNR as in Fig.10, 11 and 12. It is clear from the results that when reaching the optimum value of M both sensing matrices perform nearly the same except in some cases in Fig.11, where Randn gives slightly better performance than Hadamard. But this can be negligible when compared to the reduction in complexity gained by using Hadamard matrix which helps in accomplishing

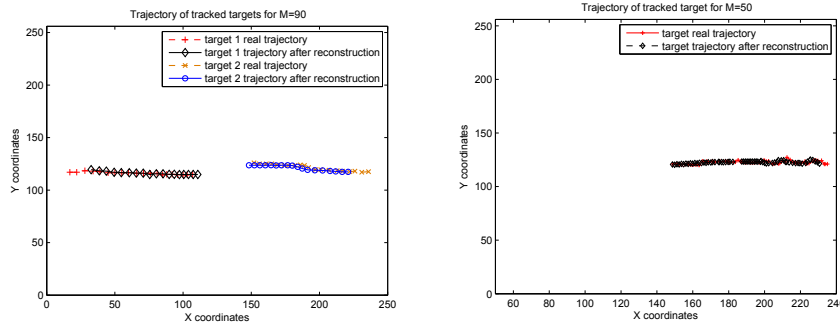
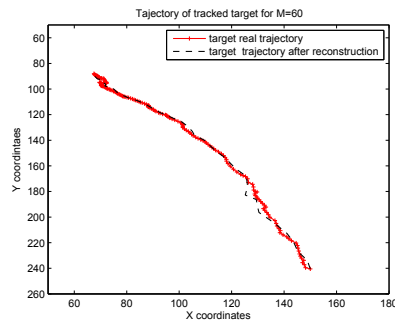
(a) Walking men dataset, $M=90$ (b) Shopping center 1, $M=50$ (c) Shopping center 2, $M=60$

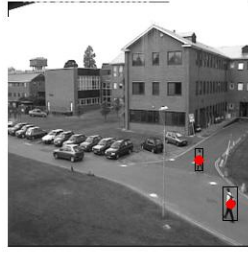
Fig. 13 Comparing trajectory of detected targets after CS reconstruction for 3 different datasets

the main objective to save sensor nodes power and as a result maximizes their lifetime.

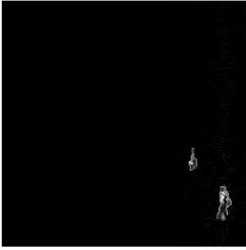
After choosing appropriate compression rates for different sparse datasets, the probability of detection $P_{d_{cs}}$ after CS and image reconstruction is analyzed to study the impact of adaptive CS on the performance of the detection problem. Fig.15 shows $P_{d_{cs}}$ for "Waking men" dataset with respect to various number of measurements M and reconstruction PSNR for a $K = 30\%$ (non-zero coefficients) dataset. The detection is tested after reconstructing compressed images using different compression rates, where various sizes of measurements are produced with different M till reaching $M = 70$ satisfying (1) and the simulation conducted above as shown in Fig.15(a). It is clear from the figures there is a direct relation between reconstruction PSNR and the size of sensing measurement matrix M (compression rates), which is reflected in Fig.15(b) where lower values of M results in low PSNR reconstructed images



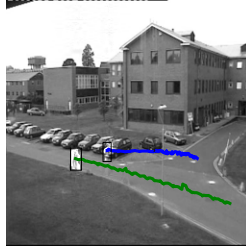
(a) detected targets



(b) only human detected targets



(c) Background subtracted frame eliminating vehicles



(d) Predicted trajectory tracking for multi-targets

Fig. 14 Comparing trajectory tracking of moving targets for dataset "4" (Walking)

and as a result low $P_{d_{cs}}$. On the other hand, as M increases the $P_{d_{cs}}$ increases till nearly reaching $\approx 100\%$ and a $35dB$ PSNR.

Fig.16 shows the $P_{d_{cs}}$ using CS for different sizes of sensing measurement matrices and different sparsity levels. As shown, for more sparse images (Less K) the probability of detection reaches $\approx 100\%$ requiring lower values of M . For instance, an image with $K = 3\%$ means that the number of nonzero elements are only 3% of the total size of the image and the remaining 97% are zeros. This is an indication that either few number of targets are present or the camera is zoomed out so the targets' size is small compared to the total scene. For an images with $K = 3\%$ the $P_{d_{cs}}$ reaches $\approx 100\%$ with $M = 40$. Whereas, with less sparse images $K = 30\%$, the value of M is increased till reaching 70 . This illustrates the save in energy by dynamically choosing the size of sensing measurement matrices according to the sparsity of images, where it

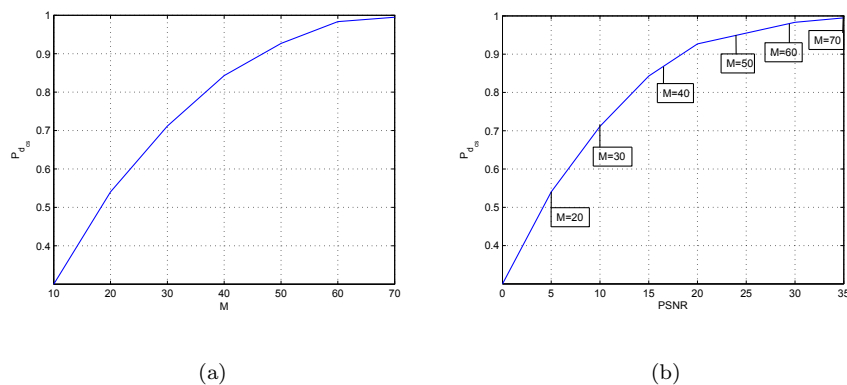


Fig. 15 Probability of detecting a target after CS reconstruction vs. (a) M and (b) reconstruction PSNR for "Walking men" dataset

will be a waste for a 97% sparse image to be compressed by projecting a sensing measurement matrix with $M = 70$ at the time it could be compressed with a sensing measurement matrix with $M = 40$ without compromising the detection probability. Furthermore, if lower values of M are used with less sparse images, CS fails to achieve a high PSNR of reconstructed images, and as a result the probability of detection is affected.

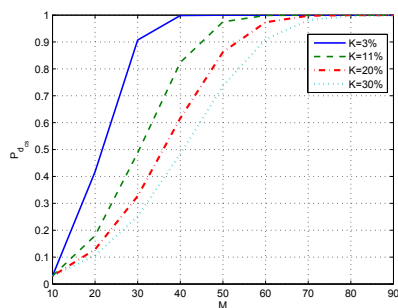


Fig. 16 Probability of detection using CS vs. M for different percentage of sparsity levels

6.4 Analysis of the Probability of missed detection for CS-based duty-cycled WWSN

Integrating the concept of CS with the detection problem might degrade the probability of detection by increasing the probability of missed detection if

choosing wrong values of M as shown in Fig.17. As previously mentioned, the values of M should be dynamically altered according to the sparsity nature of images. For illustration, Fig.17(a) and 17(b) consider different levels of sparse images $K = 30\%$ and 11% , respectively. If values of M are lower than required, the compressed image cannot be reconstructed properly, hence the probability of missing a given target increases compared to previous analysis without the integration of CS. To maintain the same probability of detection as without incorporating CS to the detection problem, CS adaptively chooses the optimum values of M according to sparsity levels. For instance, Fig.17(a) shows that for a $K = 30\%$ image, 70 measurements are required to achieve the same P_{md} , while to achieve the same performance of detection for a more sparse image ($K = 11\%$) without wasting energy of the communication channel bandwidth, Fig.17(b) shows that M is reduced to 40 measurements. If the value of M is kept constant regardless of the sparsity nature of different images two cases might occur; (i) if the value of M is lower than required, the probability of missed detection increases due to low PSNR reconstructed images, as a result affecting the performance of the detection problem, or (ii) if the value of M is higher than required, more measurements are produced whereas more compression could be applied, hence wasting communication bandwidth.

Results prove that selecting duty cycles and dynamically choosing the appropriate compression rates for different images and videos according to their sparsity nature, the same performance of detection is achieved as in [8] (before integrating adaptive CS). In addition reducing the size of transmitted data that saves more energy which is one of the main constraints in WVSNs. Hence, adaptive CS is capable of reaching the maximum compression rate per dataset without compromising the probability of detection.

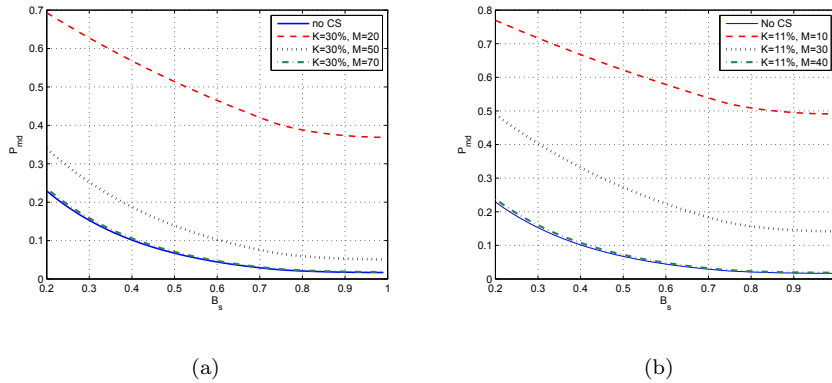


Fig. 17 Probability of missed detection with and without CS vs. different duty cycles for different sparsity levels and M (a) $K = 30\%$ and (b) $K=11\%$

Previous results presented so far refer to the cases where a single target enters the monitored area. However, analyzing the impact of multi-targets entering the monitoring area at the same time on the probability of missed detection is challenging. Analysis are carried out on the CS-integrated target detection scenario to evaluate the impact of multi-targets on the probability of missed detection, where CS adaptively chooses the value of M based on the new sparsity level of the image, as the presence of multi targets, the number of non-zero elements in the background subtracted image is expected to increase. The K and M analysis are then carried out to illustrate the impact of changing the number of targets on the probability of missed detection. It is assumed that a single sensor can detect and take a snapshot of multiple targets crossing its sensing area. Fig.18 shows the effect of various number of targets entering the sensing area at the same time in the CS scenario for a given sparsity level image and adaptively choosing value of CS measurements M . The targets enter with a velocity $v = 15m/s$, r_s is set to 50, $N = 50$ sensor nodes are deployed and t_s is set to 50sec. Fig.18(a) shows the probability of missing all incoming targets (2,4 and 6) as a function of β_s , by increasing the number of incoming targets the probability of missing all targets becomes lower than P_{md} of a single-target (solid line). While in Fig.18(b), P_{mo} is shown as a function of β_s for various number of incoming targets (2,4 and 6), it is clear that by increasing the number of monitored targets, there is a probability that at least one of the targets is not detected.

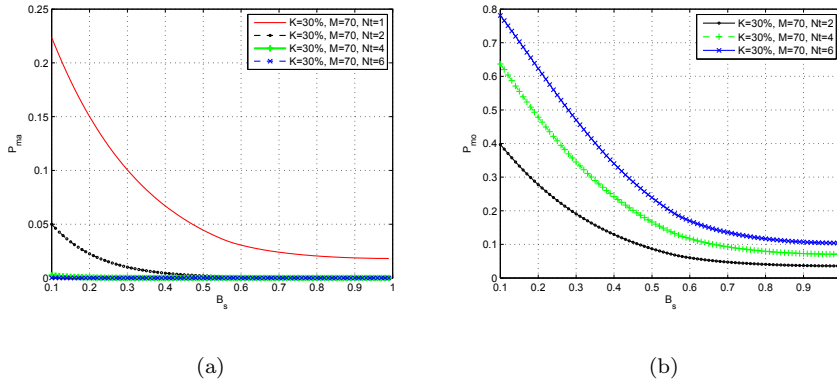


Fig. 18 Probability of missed detection vs. different duty cycles for different number of targets and for a given sparsity level and corresponding M . (a) Probability of missing all targets and (b) probability of missing at least one target

6.5 Energy complexity

To illustrate the energy saving after applying CS, we used the energy model in [35], where energy cost dissipated by a node over a distance d is denoted by E_{tx} as shown in (19).

$$E_{tx} = E_{elec} * k + e_{amp} * k * d^2 \quad (19)$$

Where, k is size of compressed data (samples) transmitted, $E_{elec} = 50nJ/bit$, is the energy being used to run transmitter and receiver circuit, $e_{amp} = 100pJ/bit$ for the transmitted amplifier.

Table 1 Transmission energy using CS, block CS and without CS for different k

Dataset with/without CS		Size of transmitted data k	Transmission Energy Etx
without CS	"Walking men"	64K	3.3mJ
	"Shopping center 1"	64K	3.3mJ
	"Shopping center 2"	64K	3.3mJ
CS	"Walking men"	17K	0.85mJ
	"Shopping center 1"	15K	0.7mJ
	"Shopping center 2"	12K	0.6mJ

In WVSNs, most energy dissipated is during the transmission and reception, in our case the reception is the base station node which is assumed not to be battery-powered. Hence minimizing transmission energy can have more impact on energy saving [36, 37] Assuming all sensor nodes have the same unit distance d from the receiver side, Table.1 shows the energy dissipated during transmission for different k (number of data samples transmitted). As illustrated, according to different k (which varies depending on compression rates due to sparsity levels), there is an average of $\approx 70\%$ energy saving as compared to transmitting the captured image without CS.

Table 2 Adaptive CS computational time for 3 datasets

Dataset	Computational time
"Walking man"	0.03s
"Shopping center1"	0.005s
"Shopping center2"	0.0055s

Table.2 summarizes the computational time for the adaptive CS process including the calibration phase and the target detection. As shown the computational time for "Shopping center1" and "Shopping center2" is less than "Walking men" due to their higher sparsity level. However these times shown include the calibration time which is only performed once per node to adjust the compression rate according to the sparsity level of the image.

7 Conclusion

The performance of target detection in WVSNS may degrade due to many factors such as node deployment, number of nodes, velocity and position of targets. Moreover, by integrating CS with the detection problem, the performance may degrade more than the desired and acceptable level. This is due to other factors such as image sparsity and, loss of information in compression. Hence, there is always a tradeoff between energy consumption (network lifetime) and detection performance. As a result, we derived the first analytical framework for the target detection problem, where the performance is tested in terms of the probability of missing a target. Experiments were tested on comprehensive standard datasets with different sparsity levels resembling indoor and outdoor scenes for single and multiple targets detection. Different sparsity levels were examined to investigate the effect of sparsity on the chosen compression rates. As a result of this framework, analysis revealed a very interesting result, that by selecting duty cycles and dynamically choosing the appropriate compression rates for different images and videos according to their sparsity nature, the desired performance of detection can be achieved with adaptive CS and at the same time saving energy. Adaptive CS is therefore a strong candidate where on average energy waste is reduced by approximately 70% as compared to transmitting the captured image without CS.

References

1. F.G.H.Yap and H.H.Yen, "A survey on sensor coverage and visual data capturing/processing/transmission in wireless visual sensor networks," *Sensors*, vol. 14, pp. 3506–3527, February 2014.
2. T.Winkler and B.Rinner, "Security and privacy protection in visual sensor networks: A survey," *ACM Computing Surveys (CSUR)*, vol. 47, no. 1, July 2014.
3. F.Wang and J. Liu, "Networked wireless sensor data collection: issues, challenges, and approaches," *Communications Surveys and Tutorials, IEEE*, vol. 99, pp. 1–15, 2010.
4. S.Soro and W.Heinzelman, "A survey on visual sensor networks," *Hindawi publishing corporation, Advances in Multimedia*, vol. 2009, no. 640386, pp. 1–21, May 2009.
5. Y.Charfi, B.Canada, N.Wakamiya, and M.Murata, "Challenges issues in visual sensor networks," in *IEEE on wireless Communications*, April 2009, pp. 44–49.
6. I.F.Akyildiz, T.Melodia, and K.R.Chowdhury, "A survey on wireless multimedia sensor networks," *computer Networks*, vol. 51, pp. 921–960, March 2007.
7. Q.Cao, T.Yan, J.Stankovic, and T.Abdelzaher, "Analysis of target detection performance for wireless sensor networks," in *In DCOSS05*, 2005, pp. 276–292.
8. P.Medagliani, J.Leguay, G.Ferrari, V.Gay, and M.Lopez-Ramos, "Energy-efficient mobile target detection in wireless sensor networks with random node deployment and partial coverage," *Pervasive and Mobile Computing*, vol. 8, no. 3, p. 429447, 2012.
9. Y.Wang and D.Wang, "Energy-efficient node selection for target tracking in wireless sensor networks," *International Journal of Distributed Sensor Networks*, vol. 2013, 2013.
10. O.Demigha, W.K.Hidouci, and T.Ahmed, "On energy efficiency in collaborative target tracking in wireless sensor network: A review," *IEEE Communications Surveys Tutorials*, vol. 15, no. 3, 2013.
11. R.Tan, G.Xing, J.Wang, and H.C.So, "Collaborative target detection in wireless sensor networks with reactive mobility," in *16th International Workshop on Quality of Service IWQoS*, June 2008, pp. 150–159.

12. E.J.Candes and M.B.Wakin, "An introduction to compressive sampling," *IEEE Signal Processing Magazine*, pp. 21–30, March 2008.
13. D. Donoho, "Compressed sensing," *IEEE Transactions on Information Theory*, vol. 52, no. 4, pp. 1289–1306, 2006.
14. M.Zhao, A.Wang, B.Zeng, L.Liu, and H.Bai, "Depth coding based on compressed sensing with optimized measurement and quantization," *Ubiquitous International Journal of Information Hiding and Multimedia Signal Processing*, vol. 5, no. 3, pp. 475–484, July 2014.
15. C.Patsakis and N.G.Aroukatos, "Lsb and dct steganographic detection using compressive sensing," *Ubiquitous International Journal of Information Hiding and Multimedia Signal Processing*, vol. 5, no. 4, pp. 20–32, January 2014.
16. V.Cevher, A.Sankaranarayanan, M. Duarte, D.Reddy, R. Baraniuk, and R.Chellappa, "Compressive sensing for background subtraction," 2008.
17. A.Mahalanobis and R.Muise, "Object specific image reconstruction using a compressive sensing architecture for application in surveillance systems," *IEEE Transactions on Aerospace and Electronic Systems*, vol. 45, no. 3, pp. 1167–1180, July 2009.
18. C.T.Chou, R.Rana, and W.Hu, "Energy efficient information collection in wireless sensor networks using adaptive compressive sensing," in *IEEE 34th Conference on Local Computer Networks (LCN)*, Zurich, Switzerland, October 2009, pp. 443–450.
19. E.J.Candes and B.Recht, "Exact matrix completion via convex optimization," *CoRR*, vol. abs/0805.4471, 2008.
20. S.Fayed, S.M.Youssef, A.El-Helw, M.Patwary, and M.Moniri, "Adaptive compressive sensing for target tracking within wireless visual sensor networks-based surveillance applications," *Multimedia Tools and Applications*, vol. 75, no. 11, pp. 6347–6371, 2016.
21. R. Baraniuk, "Compressive sensing," *IEEE Signal Processing Magazine*, pp. 118–124, July 2007.
22. E. Wang, J. Silva, and L. Carin, "Compressive particle filtering for target tracking," in *IEEE/SP 15th Workshop on Statistical Signal Processing, SSP*, September 2009, pp. 233–236.
23. J.Romberg, "Imaging via compressive sampling," *IEEE Signal Processing Magazine*, pp. 14–20, March 2008.
24. H. C. Huang and F. C. Chang, "Robust image watermarking based on compressed sensing techniques," *Journal of Information Hiding and Multimedia Signal Processing*, vol. 5, no. 2, pp. 275–285, April 2014.
25. E.J.Candes, "Compressive sampling," in *Proc. of the International Congress of Mathematicians*, 2006.
26. A.Hormati, O.Roy, Y.M.Lu, and M.Vetterli, "Distributed sampling of signals linked by sparse filtering: theory and applications," *IEEE Transactions on Signal Processing*, vol. 58, no. 3, pp. 1095–1109, March 2010.
27. J. Tropp and A. Gilbert, "Signal recovery from random measurements via orthogonal matching pursuit," *IEEE Transactions on Information Theory*, vol. 53, no. 12, pp. 4655–4666, December 2007.
28. P.Medagliani, J.Leguay, V.Gay, M.Lopez-Ramos, and G.Ferrari, "Engineering energy-efficient target detection applications in wireless sensor networks," in *IEEE International Conference on Pervasive Computing and Communications (PerCom)*, March 2010, pp. 31–39.
29. Z.Wang, G.R.Arce, B.M.Sadler, J.L.Paredes, and X. Ma, "Compressed detection for pilot assisted ultra-wideband impulse radio," in *IEEE International Conference on Ultra-Wideband ICUWB*, September 2007, pp. 393–398.
30. M.A.Davenport, M.B.Wakin, and R.G.Baraniuk, "Detection and estimation with compressive measurements," Rice University, Department of ECE, Technical Report, Tech. Rep., 2006.
31. F. Cheng and Y. Chen, "Real time multiple objects tracking and identification based on discrete wavelet transform," *Elsevier Pattern Recognition Journal*, vol. 39, p. 1126–1139, 2006.
32. "Caviar datasets," Dataset: EC Funded CAVIAR project/IST 2001 37540, <http://homepages.inf.ed.ac.uk/rbf/CAVIAR/>, 2001.
33. Y.Wu, J.Lim, and M.Yang, "Visual tracker benchmark," <https://sites.google.com/site/trackerbenchmark/benchmarks/v10>, 2013.

34. H. Jiang, W. Deng, and Z. Shen, "Surveillance video processing using compressive sensing," *arXiv preprint arXiv:1302.1942*, 2013.
35. Ms.V.MuthuLakshmi, "Advanced leach protocol in large scale wireless sensor networks," *International Journal of Scientific and Engineering Research*, vol. 4, no. 5, pp. 248–254, May 2013.
36. A.Redondi, D.Buranapanichkit, M.Cesana, M.Tagliasacchi, and Y.Andreopoulos, "Energy consumption of visual sensor networks: Impact of spatio-temporal coverage," *IEEE tranaction on Circuits and Systems for Video Technology*, vol. 24, no. 12, pp. 2117–2131, December 2014.
37. P.Mohanty, M.R.Kabat, and M.K.Patel, "Energy efficient transmission control protocol in wireless sensor networks," in *Wireless Networks and Computational Intelligence*, ser. Communications in Computer and Information Science. Springer Berlin Heidelberg, 2012, vol. 292, pp. 56–65.